Smart Structures and Systems, *Vol. 27, No. 6 (2021) 943-950*
DOI: https://doi.org/10.12989/sss.2021.27.6.943

Simulation and experimental study on MFL-based damage detection capability considering velocity condition for railroad NDE

Ju-Won Kim [1], Jooyoung Park [2], Donghoon Kang [3] and Seunghee Park*[2,4]

[1] *Department of Safety Engineering, Dongguk University-Gyeongju, Gyeongju, Gyeongsangbuk-do, 38066, Republic of Korea*
[2] *School of Civil, Architectural Engineering and Landscape Architecture, Sungkyunkwan University, Suwon, Gyeonggi-do 16419, Republic of Korea*
[3] *Railroad Major Accident Research Team, Korea Railroad Research Institute, Uiwang, Gyeonggi-do, 16105, Republic of Korea*
[4] *Technical Research Center, Smart Inside AI Co., Ltd., Suwon, Gyeonggi-do 16419, Republic of Korea*

(*Received September 3, 2019, Revised January 12, 2021, Accepted April 10, 2021*)

Abstract. This paper used a magnetic flux leakage (MFL) method compatible with steel structures to analyze quantitative change in a leakage signal due to defects on the surface of a railroad. A numerical simulation using a two-dimensional finite element method (2D-FEM) was used to analyze MFL signals from defects on the railroad. An experiment was then carried out to investigate the capability of the MFL-based non-destructive evaluation (NDE). We also focused on the velocity effect of the MFL signals by analyzing the magnetic hysteresis phenomenon. The quantitative change in leakage signals was determined by selecting depth of the defect and inspection velocity as parameters in a simulation and in an experiment. The MFL signals obtained showed variations that were simultaneously affected by inspection velocity and defect depth. MFL-based damage detection in a railroad is conclusively confirmed to be sufficiently feasible within the range of operational speeds of an inspection train.

Keywords: railroad inspection; magnetic flux leakage; local damage detection; velocity effect; non-destructive evaluation

1. Introduction

Recently, various methodologies and inspection techniques have been used to inspect local damage in critical members of structures to overcome the limitations of whole-structure monitoring. In particular, non-destructive testing (NDT) for structural health monitoring (SHM) has been widely used to inspect and assess the structural condition with regard to damage.

Railroads are vital components of railway services and must withstand and distribute the weight of a train to the ground. A railroad has the advantage of producing small vibrations due to the considerably high stresses on relatively small areas at which wheels of the train make contact.

However, stress can create plastic deformation on the railroad, resulting in various types of damage (Sawadisavi 2010). Damage to the railroad spreads rapidly to the entire structure as time passes and can lead to disasters, including derailments in severe cases (Barke and Chiu 2005). Accordingly, it is important to detect damaged rails at an early stage (Dey *et al*. 2016, Fadaeifard *et al*. 2013).

Magnetic flux leakage (MFL) is a widely used conventional NDE technique that can be applied for high-speed inspections. The method is applicable to many types of steel structures, including railroads, pipelines, and plate-like structures (Zhang *et al*. 2009, Shi *et al*. 2015, Kim *et al*. 2018, Kim and Park 2017, 2018).

Many studies have been conducted to develop damage detection methods of steel structures using MFL-based NDE. Those studies have verified the feasibility of using the technique to detect damage to target objects. In most cases, however, the specimens used for damage detection were limited to pipelines and plate-like structures (Ahmad *et al*. 2015, Arifin *et al*. 2015, Feng *et al*. 2017, Tsukada *et al*. 2010). Few studies have used railroads as target objects (Chen *et al*. 2011).

Although the MFL method is highly capable of detecting damage, it is still fraught with problems when used in conjunction with high-speed inspection because damage detection was carried out in a static state in most previous studies (Lukyanets *et al*. 2003, Sun and Kang 2010, Al-Naemi *et al*. 2006). Static-state damage detection can bring about difficulties in interpreting MFL signals obtained through an inspection. Moreover, several previous studies presented differing opinions regarding variations in the magnitudes of MFL signals when considering the inspection velocity (Wang *et al*. 2014, Li *et al*. 2006).

In addition, some investigations of MFL signals obtained from damaged structures have used numerical simulations based on two-dimensional (2-D) or 3-D models with the finite element method (FEM) but have not performed experimental studies (Wu *et al*. 2015, Dutta *et al*. 2009). However, results without experimental verification can produce an inaccurate diagnosis of the damage.

*Corresponding author, Ph.D., Professor,
E-mail: shparkpc@skku.edu

ISSN: 1738-1584 (Print), 1738-1991 (Online)

This paper presents a simulation and experimental study using an MFL-based NDE technique. The damage detection capability was investigated for the railroad under different inspection velocities. To identify the magnitude of the MFL signals due to the presence of damage and variation in inspection velocity, a 2-D FEM model was produced. The analyses were performed using the transient analysis method. An experimental study was then conducted with MFL-based NDE equipment. Finally, the damage detection capability for the railroad and the effect of the inspection velocity on the MFL signals were verified by comparing the results of the simulation and the experiment.

2. Principle of the MFL-based NDE Technique

2.1 Principle of sensing MFL signals

Leakages in magnetic fields occur on the surface or subsurface of a ferromagnetic material when the local thickness is significantly reduced. In Fig. 1(a), there are no magnetic flux lines over the surface of the specimen, so they cannot reach the sensor. In Fig. 1(b), however, there is a reduction in the thickness of the specimen, which results in an internal magnetic field that allows the flux lines to leak from the surface around the defects (Cho 2011, Bubenik *et al*. 1992). The leaked flux can be detected by a Hall sensor, which consists of a transducer for which the output voltage varies in response to the applied magnetic fields (Ramsden 2006). Consequently, the leakage signal is acquired in the voltage output (Park *et al*. 2014).

2.2 Velocity effect on MFL signals

When the acquired MFL signals are interpreted, the velocity effect on the signals is crucial in that it can change the magnitude of the signals. This can lead to misinterpretations of signals when estimating the level of damage.

The changes in MFL signal due to the increase in velocity can be easily understood in terms of the magnetization process, as represented by the following Eqs. (1) and (2).

$$\mathrm{M} = \chi_v H \tag{1}$$

$$\mathrm{B} = \mu_0(H + M) = \mu_0(1 + \chi_v)H = \mu H \tag{2}$$

Here, M, H, B, χ_v, μ_0, and μ represent the magnetization of the ferromagnetic material, the magnetic field strength, the magnetic flux density, the magnetic susceptibility, the permeability of air, and the permeability of the material, respectively (O'Handley 1999).

If magnetic fields are applied to a ferromagnetic specimen and the applied fields are revoked from it, the specimen retains magnetism. The residual magnetism is related to migration of the magnetic domain wall (Jiles and Atherton 1984, Hauser 1994, Cullity and Gragam 2011). However, if magnetization is considered as a dynamic process, the total time of the magnetization will decrease due to the increase in velocity. A decrease in magnetization time can cause a reduction in magnetic susceptibility, which is a dimensionless proportionality constant that indicates the degree of magnetization of a material in response to an applied magnetic field. Therefore, the permeability of the material decreases with susceptibility based on Eq. (2).

The decrease in permeability has an important implication regarding the amount of magnetic flux flowing into the ferromagnetic material. The amount of flux flowing under the surface decreases due to the decrease in permeability. This phenomenon can be explained by Ohm's law, which describes current flows. Similar to the way an electric field causes an electric current to follow the path of least resistance, a magnetic field causes magnetic flux to take the path of least magnetic reluctance (Nilsson and Riedel 2008). Thus, the leaked flux on the surface defects of the material increases due to the increase in velocity.

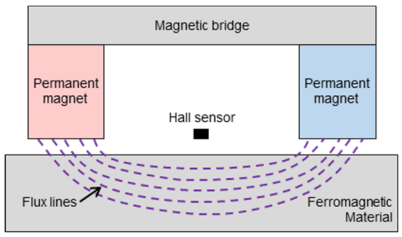

(a) Intact specimen

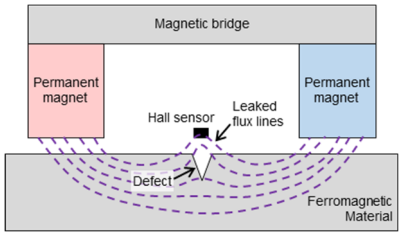

(b) Damaged specimen

Fig. 1 Principle of MFL-based damage detection

3. Numerical simulation

3.1 Simulation setup

As illustrated in Fig. 2, the model is set up in 2-D, with X-Y coordinates representing the cross-section of the MFL probe and specimen. Table 1 shows the properties of the simulation model that comprises a magnetization part and a sensing part. A magnetic bridge (magnetization part) incorporating a yoke and two permanent magnets with different poles were modeled so that the flux lines traveled through the structures. Steel was adopted as the ferromagnetic material for the yoke and the specimen, as it has a non-linear B-H curve that can account for the magnetic hysteresis phenomenon.

The sensing part containing the Hall sensor is in the middle between the two permanent magnets.

A railroad specimen was also modeled. However, it includes only the head of the rail because that is where the sensor is located. Moreover, the magnetic fields induced by the magnets seldom affect the lower part of the rail.

In this simulation, defect depth (d) and inspection velocity (v) were chosen as parameters to investigate the

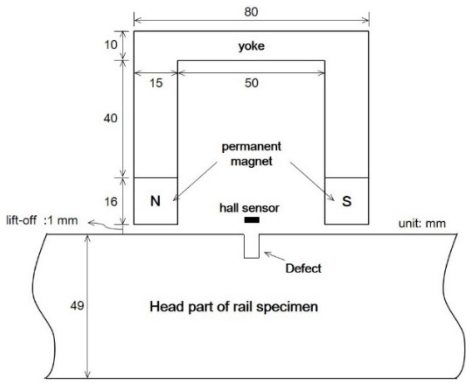

Fig. 2 Simulation model of railhead and magnetization part

Table 1 Properties of the simulation model

Components	Properties	
Permanent magnets	Materials	Neodymium (NdFe 35)
	Permeability	1
	Conductivity	6.25e5 S/m
	Coercivity	-8.9e5 A/m
Magnetizer	Materials	Carbon steel
	Permeability	nonlinear B-H curve
	Conductivity	2e6 S/m
Rail specimen	Materials	Steel_1008
	Permeability	nonlinear B-H curve
	Conductivity	2e6 S/m
Defect	Materials	Rectangular air slot
	Permeability	1
	Conductivity	0 S/m

changes in MFL signals due to changes in those parameters. A transient analysis was adopted to reflect the relative movement between the magnetization part and the specimen. For the parameters, the depth of the defect and the inspection velocity ranged from 1 to 5 mm and from 1 to 3 m/s, respectively. These velocities are within the range of the movement speed of the linear movement device for the experiment.

The Hall sensor used to detect the MFL signals senses the y component of the magnetic flux density (B). Hence, the MFL signals obtained in the simulation were presented in terms of the y component of the magnetic flux density (B_y).

3.2 Magnetic flux density due to defects

The simulated MFL results due to the increases in defect depth and inspection velocity are shown in Figs. 3-5, where the values of the x axis and y axis on the graph represent the position of the Hall sensor from the center of the defect and the By, respectively.

All of the simulated MFL signals indicate the same pattern in which the magnitude of By initially decreases noticeably, after which there is a rapid increase. Therefore,

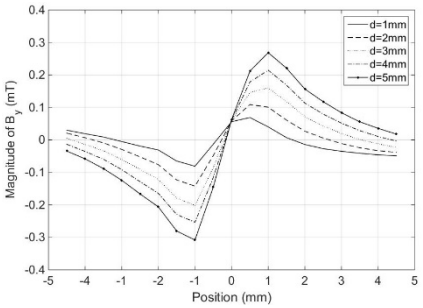

Fig. 3 B_y due to change in depth (v = 1 m/s)

the By curves have two peak values on both sides of the position of the Hall sensor. To indicate the magnitude of MFL signals quantitatively, the vertical distance between two peaks (By, pp), commonly called peak to peak value (P-P value), has been utilized as an index in this study.

The change of magnetic flux density from the simulation analysis was identified due to the change of defect depth with inspection velocity 1m/s and is plotted in Fig. 3.

At the same velocity condition, greater leakage magnetic flux is generated with increasing depth of damage. Therefore, the extracted B_y value quantified from the magnetic flux signal increased stepwise from 0.15 mT to 0.577 mT when damage depth increased from 1 mm to 5 mm.

MFL signal magnitudes and variations were also obtained at a higher inspection velocity. Thus, the results of the two inspection velocities of 2 m/s and 3 m/s were obtained, as correspondingly illustrated in Figs. 4 and 5.

Even at inspection velocities of 2 m/s and 3 m/s, identical curve shapes are shown for the case where v = 1

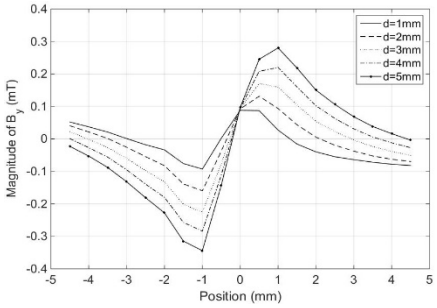

Fig. 4 B_y due to change in depth (v = 2 m/s)

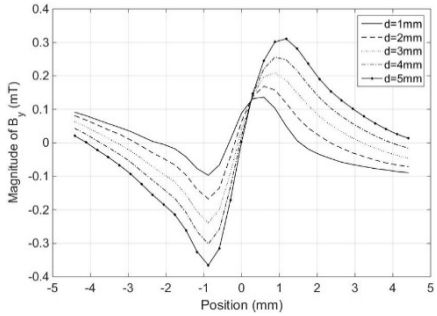

Fig. 5 B_y due to change in depth (v = 3 m/s)

Table 2 Numerical value of $B_{y,pp}$ due to changes in *d* and *v* (mT)

d (mm) \ v (m/s)	1	2	3
1	0.150	0.202	0.262
2	0.251	0.309	0.360
3	0.362	0.408	0.469
4	0.468	0.512	0.570
5	0.577	0.624	0.680

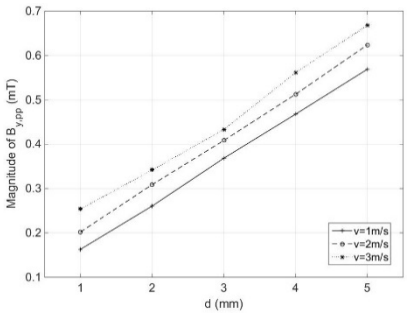

Fig. 6 $B_{y,pp}$ due to changes in depth and velocity

m/s. Also, as in the case of 1 m/s, simulation results in 2 m/s and 3 m/s showed the same pattern, in which By increases as the depth of damage becomes deeper. In addition, under the same damage depth condition, a greater By value was detected as inspection velocity increased. Table 2 and Fig. 6 present the numerical values of $B_{y,pp}$ for each damage depth and inspection velocity case.

In Table 2 and Fig. 6, the $B_{y,pp}$ values showed a pattern that increases linearly with an increase in depth of the defect. And the $B_{y,pp}$ values increased at all defect depth levels due to the increase in diagnostic velocity condition. Consequently, through the results of the MFL-based simulation, the increase in magnitude of the detected magnetic leakage signals was confirmed according to the increase in damage depth and inspection velocity.

4. Experimental study

4.1 Experimental setup

As shown in Fig. 7, the test setup for the MFL-based railroad damage inspection consists of a 14-ch sensor head equipped with a magnetization part and a sensing part, a rail specimen, a compact data-acquisition (DAQ) device, a terminal board, a linear movement device, and a laptop computer. The compact DAQ and terminal board were correspondingly used for data acquisition and signal processing, and the obtained data was then analyzed using the laptop computer. To investigate the velocity effect, a linear movement device was specially designed and fabricated for the railroad damage inspection. The relative velocity between the specimen and the sensor head was generated by a controller that causes the sensor head to move linearly on the specimen at a constant velocity of

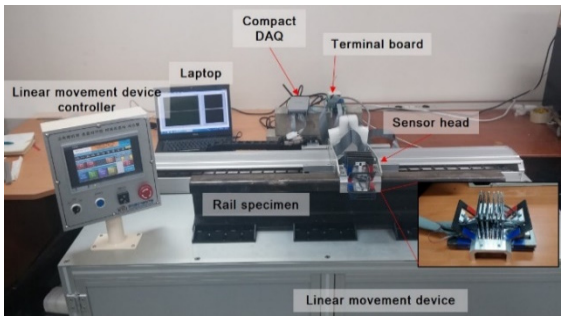

Fig. 7 Experimental setup for the MFL-based railroad NDE

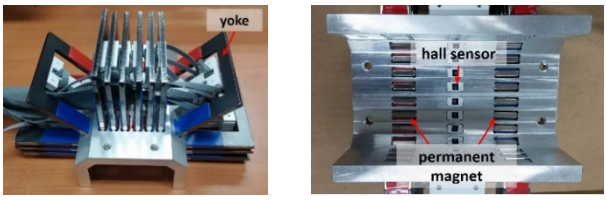

(a) Bird view of sensor head (b) Bottom view of sensor head

Fig. 8 Multi-channel MFL sensor head

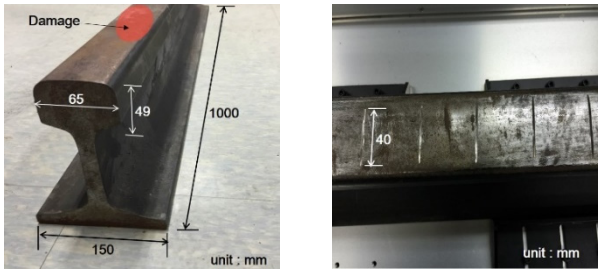

(a) Rail specimen (b) Damage on rail head

Fig. 9 Specifications of rail specimen and fabricated damage

1 m/s to 3 m/s, which are the same velocity conditions used in the simulation analysis.

The sensor head comprises the magnetization part and the sensing part, which have the same configuration as in the simulation model, as shown in Fig. 8. The number of sensing channels of the sensor head is 14, and each sensing channel has a Hall sensor to measure the magnetic flux signal and a set of permanent magnet yoke to magnetize the rail specimen.

The rail specimen was used for damage inspection, and the various size damages were formed artificially on the rail head as shown in Fig. 9. The length of the rail specimen was 1 m, and width and height of the rail head were 65mm and 49 mm.

Five cracks with depths ranging from 1 to 5 mm were produced along the rail specimen in the same manner as in the simulation. The width and the length were fixed at 1.5 mm and 40 mm, respectively. The damage was located at regular intervals of 50 mm. A side view and the dimensions of the damage are illustrated in Fig. 10.

Each Hall sensor had a hall element that was perpendicular to the surface of the rail head so that the y

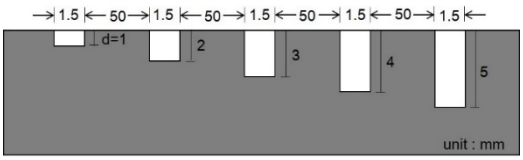

Fig. 10 Side view of the damage

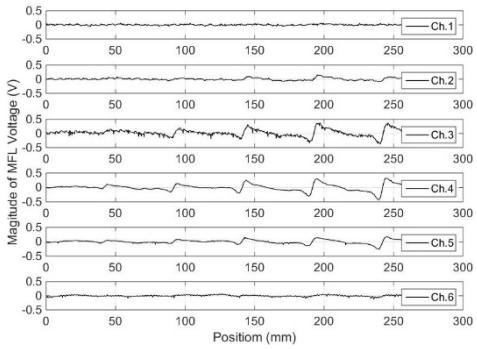

Fig. 11 MFL signals obtained from 6 channels

component of the MFL signals could be detected by the Hall effect. The measurement was repeated 25 times, and the sampling frequency was 5 kHz each time.

4.2 MFL voltage due to defects

The magnetic flux signals collected from the multi-channel MFL sensor head are shown in Fig. 11. In this study, signals from only 6 sensing channels passing through the upper surface of the rail head where the damage is located were used for the experiment.

In Fig. 11, four (from Ch. 2 to Ch. 5) of the six channels showed damage signal patterns similar to those in the simulation. Therefore, the mean value of the signals from four channels was calculated and used for each case of damage. These calculations were also adopted for the remaining velocity cases.

The MFL signals measured at each damage depth are superimposed and plotted on Figs. 12-14 for each inspection velocity condition.

The magnitudes of the y component of the MFL signals showed patterns analogous to the results of the simulation. Two peak values were also found in the curve, as in the simulation, and the vertical distance between the two peaks (MFL_{pp}) increased with depth of the defect, while the horizontal distance between the two peaks did not change. The results at inspection velocity of 2 m/s and 3 m/s are illustrated in Figs. 13 and 14, respectively.

The magnitudes of the MFL signals were different significantly when the inspection velocity was 2 m/s and 3 m/s, but the shape of the MFL signals was maintained. When the velocity was increased to 2 m/s and 3 m/s, the output voltage that reflect the magnetic flux was measured higher than 1 m/s velocity condition at all damage depth condition.

The MFL signals obtained from all inspection cases were compared to each other. The P-P value for each velocity and depth condition was extracted. Each P-P value

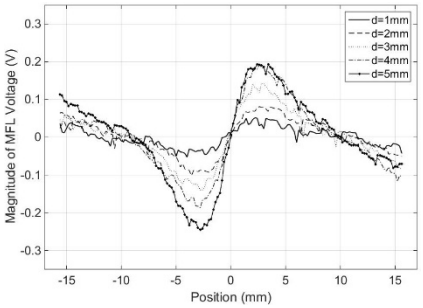

Fig. 12 MFL signals due to changes in d (v = 1 m/s)

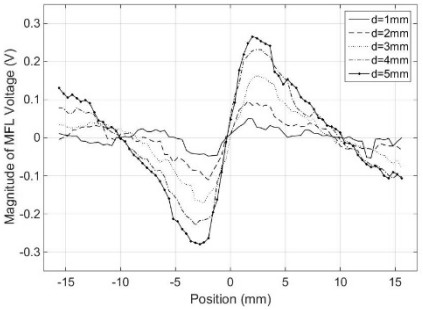

Fig. 13 MFL signals due to changes in d (v = 2 m/s)

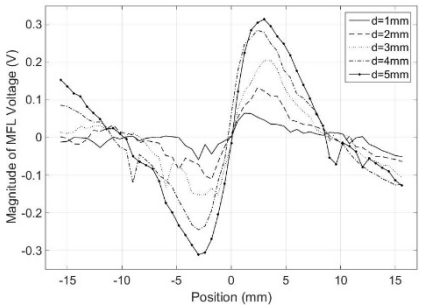

Fig. 14 MFL signals due to changes in d (v = 3 m/s)

was the average of 25 experiments. These are shown in Table 3 and Fig. 15.

Similar to the simulation results, the P-P value increased proportionally as the depth of damage increased. The P-P value of MFL also increased regularly as inspection velocity increased.

As shown in Table 3 and Fig. 15, results of the experimental study showed signal patterns pertaining to the magnitude of MFL signal analogous to the simulation results.

Table 3 Experimental results of $B_{y,pp}$ due to changes in d and v (V)

d (mm) \ v (m/s)	1	2	3
1	0.104	0.098	0.123
2	0.183	0.207	0.242
3	0.282	0.334	0.357
4	0.380	0.461	0.530
5	0.438	0.545	0.625

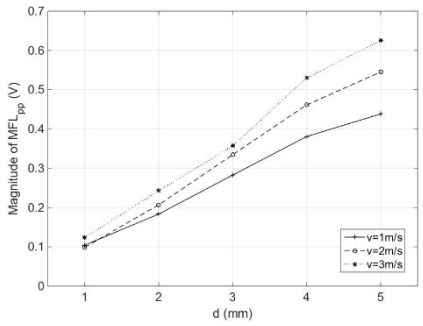

Fig. 15 MFL_{pp} due to changes in d and v

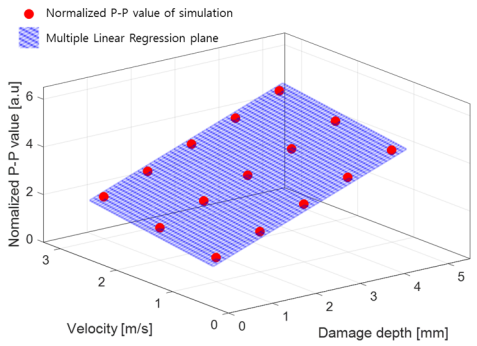

Fig. 16 Normalized P-P value and multiple linear regression plane of the simulation analysis

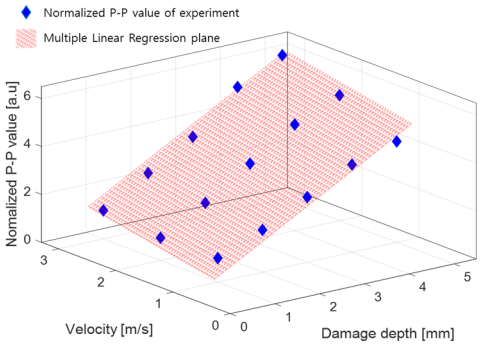

Fig. 17 Normalized P-P value and the multiple linear regression plane of the experiment

5. Comparison between the simulation and experimental results

Through simulation analysis and experimental verification of the previous section, it was confirmed that it is possible to diagnose railway damage using a leakage magnetic flux technique. It was also confirmed that the magnitude of the MFL signal increases with damage depth and inspection velocity.

A comparison analysis between the results of the simulation and the experiment was carried out to investigate the trend of change in MFL signals due variations in depth of the defect and inspection velocity. For accurate quantitative comparisons, the units of the two results were matched through the normalization process.

Normalization process by multiplying constant values was conducted by changing the normalized magnitude of MFL signal to 1 when the defect had a depth and inspection velocity of 1 mm and 1 m/s, respectively.

Table 4 presents the relative values calculated for the remaining cases in the simulation and experiment, where the value indicates the normalized magnitude of MFL_{pp}.

Through a relative comparison, the experimental results were shown to be more sensitive to depth variation of damage than the simulation results. Also, the influence of inspection velocity was greater in the experiment.

Table 4 Normalized magnitude of MFL signals

	d (mm)	v (m/s)		
		1	2	3
Simulation	1	1.000	1.347	1.747
	2	1.673	2.060	2.400
	3	2.413	2.720	3.127
	4	3.120	3.413	3.800
	5	3.847	4.160	4.533
Experiment	1	1.000	0.947	1.187
	2	1.762	1.988	2.331
	3	2.714	3.213	3.428
	4	3.657	4.430	5.092
	5	4.209	5.236	6.005

*The value is '1' when d and v are 1 mm and 1 m/s, respectively

To identify trends in depth and velocity for each analysis method, normalized P-P values (NPP) and multiple linear regression planes are shown in Figs. 16 and 17. The multiple regression equations were derived as Eqs. (3) and (4).

$$NPP_{SIM} = 0.7031D + 0.3554V - 0.0627 \quad (3)$$

$$NPP_{EXP} = 1.058D + 0.4701V - 0.9666 \quad (4)$$

Comparing Figs. 16 and 17 and Eqs. (3) and (4) shows that the change rate of normalized P-P value with increasing depth of damage is larger in the experimental study (1.058) than in the simulation (0.7031). In addition, sensitivity to inspection velocity was 0.4701 in the experimental study and 0.3544 in the simulation, indicating that the influence of the inspection velocity was more sensitive in the experimental study.

Comparison of experimental and simulation results showed that the two approaches had similar trends in the correlation of depth of damage and inspection velocity. However, some difference in the degree of sensitivity was observed between the two approaches, indicating the need for a calibration algorithm to correct this.

6. Conclusions

This study conducted a numerical simulation and an experimental investigation using an MFL-based NDE

technique. The following can be stated based on the findings of the study.

- The capability of MFL-based railroad damage detection was confirmed through signals obtained from defects near the railhead.
- The magnitude of MFL signals was verified to depend on the characteristics of the damage and the inspection velocity in the simulation study.
- B_y in the simulation study increased due to changes in depth of the defect or inspection velocity.
- The signal magnitude of MFL voltage in the experimental study showed signal patterns similar to those in the simulation.
- The MFL signals increased by 453.3% and 600.5% in the simulation and the experiment, respectively, according to the variations in depth of the defects and inspection velocity.

In this study, the possibility of MFL-based railroad diagnosis was confirmed through simulation and experimental studies. The results of the simulation and experimental study were in good agreement regarding the MFL signal pattern, though there were some differences in the amount of MFL signals. This illustrates that damages on the railroad can be accurately detected through the MFL signal generated on the damaged point.

Since the sensitivity of the MFL signal varies depending on the size of the damage, quantitative diagnosis and determination of the presence or absence of damage are possible using the MFL technique. In addition, since there is a difference in sensitivity of the signal due to the influence of inspection velocity, railroad diagnosis must consider the velocity. Therefore, it is necessary to develop a calibration method that can compensate the effect of velocity.

To develop an MFL-based NDE technique from the conclusions in this study, further research is currently underway to quantify the MFL signals so that a damage index can be drawn. In addition, algorithms to classify the damage type using a pattern recognition technique, which is increasingly being used in many applications, are in development. As a concluding remark, we put forward that the findings from this study can be applied to characterize and visualize damage on various types of steel structures such as steel beams and wire rope.

Acknowledgments

The research described in this paper was supported by the Dongguk University Research Fund of 2020.

References

Ahmad, M.I.M., Arifin, A., Abdullah, S., Jusoh, W.Z.W. and Dingh, S.S.K. (2015), "Fatigue crack effect on magnetic flux leakage for A283 grade C steel", *Steel Compos. Struct., Int. J.*, **19**(6), 1549-1560. https://doi.org/10.12989/scs.2015.19.6.1549

Al-Naemi, F.I., Hall, J.P. and Moses, A.J. (2006), "FEM modelling techniques of magnetic flux leakage-type NDT for ferromagnetic plate inspections", *J. Magn. Magn. Mater.*, **304**(2), 790-793. https://doi.org/10.1016/j.jmmm.2006.02.225

Arifin, A., Jusoh, W.Z.W., Abdullah, S., Jamaluddin, N. and Arffin, A.K. (2015), "Investigating the fatigue failure characteristics of A283 Grade C steel using magnetic flux detection", *Steel Compos. Struct., Int. J.*, **19**(3), 601-614. https://doi.org/10.12989/scs.2015.19.3.601

Barke, D. and Chiu, K.W. (2005), "Structural health monitoring in the railway industry", *Struct. Health Monit.*, **4**(1), 81-94. https://doi.org/10.1177/1475921705049764

Bubenik, T.A., Nestleroth, J.B., Eiber, R. and Saffell, B.F. (1992), "Magnetic Flux Leakage (MFL) Technology for Natural Gas Pipeline Inspection", PB-93-181899/XAB, Gas Research Institute.

Chen, Z., Xuan, J., Wang, P., Wang, H. and Tian, G. (2011), "Simulation on high speed rail magnetic flux leakage inspection", *IEEE International Instrumentation and Measurement Technology Conference*, Binjiang, Hangzhou, China, May.

Cho, S.-H. (2011), "A Study on MFL and EMAT Techniques for Intelligent Pig System for Inspection Gas Pipelines", Ph.D. Dissertation; Sungkyunkwan University, Suwon, Korea.

Cullity, B.D. and Gragam, C.D. (2011), *Introduction to Magnetic Materials*, Wiley, Hoboken, NJ, USA.

Dey, A., Kurz, J. and Tenczynski, L. (2016), "Detection and evaluation of rail defects with nondestructive testing methods", *Proceedings of the 19th World Conference on Non-Destructive Testing 2016*, Munich, Germany, June.

Dutta, S.M., Ghorbel, F.H. and Stanley, R.K. (2009), "Simulation and analysis of 3-D magnetic flux leakage", *IEEE Trans. Magn.*, **45**(4), 1966-1972. https://doi.org/10.1109/TMAG.2008.2011896

Fadaeifard, F., Toozandehjani, M., Mustapha, M. and Matori, K.A. (2013), "Rail inspection technique employing advanced nondestructive testing and Structural Health Monitoring (SHM) approaches-A review", *Malaysian International NDT Conference and Exhibition*, Kualalampur, Malaysia, January.

Feng, J., Li, F., Lu, S., Liu, J. and Ma, D. (2017), "Injurious or noninjurious defect identification from MFL images in pipeline inspection using convolutional neural network", *IEEE Trans. Instrum. Meas.*, **66**(7), 1883-1892. https://doi.org/10.1109/TIM.2017.2673024

Hauser, H. (1994), "Energetic model of ferromagnetic hysteresis", *J. Appl. Phys.*, **75**(5), 2584-2597. https://doi.org/10.1063/1.356233

Jiles, D.C. and Atherton, D.L. (1984), "Theory of ferromagnetic hysteresis", *J. Appl. Phys.*, **55**(6), 2115-2120. https://doi.org/10.1063/1.333582

Kim, J.-W. and Park, S. (2017), "Magnetic flux leakage-based local damage detection and quantification for steel wire rope non-destructive evaluation", *J. Intel. Mat. Syst. Str.*, **29**(17), 3396-3410. https://doi.org/10.1177/1045389X17721038

Kim, J. -W. and Park, S. (2018), "MFL sensing and ANN pattern recognition based automated damage detection and quantification for wire rope NDE", *Sensors*, **18**(1), 109. https://doi.org/10.3390/s18010109

Kim, J.-W., Park, M., Kim, J. and Park, S. (2018), "Improvement of MFL sensing–based damage detection and quantification for steel bar NDE", *Smart. Struct. Syst., Int. J.*, **22**(2), 239-247. https://doi.org/10.12989/sss.2018.22.2.239

Li, Y., Tian, G.Y. and Ward, S. (2006), "Numerical simulation on magnetic flux leakage evaluation at high speed", *NDT E Int.*, **39**(5), 367-373. https://doi.org/10.1016/j.ndteint.2005.10.006

Lukyanets, S., Snarskii, A., Shamonin, M. and Bakaev, V. (2003), "Calculation of magnetic leakage field from a surface defect in a linear ferromagnetic material: an analytical approach", *NDT E Int.*, **36**(1), 51-55.

https://doi.org/10.1016/S0963-8695(02)00071-3
Nilsson, J.W. and Riedel, S.A. (2008), *Electric Circuits*, Pearson, Upper Saddle River, NJ, USA.
O'Handley, R.C. (1999), *Modern Magnetic Materials*: *Principles and Applications*, Wiley, Hoboken, NJ, USA.
Park, S., Kim, J.-W., Lee, C. and Lee, J.-J. (2014), "Magnetic flux leakage sensing-based steel cable NDE technique", *Shock Vib*. https://doi.org/10.1155/2014/929341
Ramsden, E. (2006), *Hall-Effect Sensors*: *Theory and Applications*, Newnes, Burlington, MA, USA.
Sawadisavi, S.V. (2010), "Development of machine-vision technology for inspection of railroad track", M.S. Thesis; University of Illinois at Urbana-Champaign, IL, USA.
Shi, Y., Zhang, C., Li, R., Cai, M. and Jia, G. (2015), "Theory and application of magnetic flux leakage pipeline detection", *Sensors*, **15**(12), 31036-31055. https://doi.org/10.3390/s151229845
Sun, Y. and Kang, Y. (2010), "A new MFL principle and method based on near-zero background magnetic field", *NDT E Int*., **43**(4), 348-353. https://doi.org/10.1016/j.ndteint.2010.01.005
Tsukada, K., Yoshioka, M., Kawasaki, Y. and Kiwa, T. (2010), "Detection of back-side pit on a ferrous plate by magnetic flux leakage method with analyzing magnetic field vector", *NDT E Int*., **43**(4), 323-328. https://doi.org/10.1016/j.ndteint.2010.01.004
Wang, P., Gao, Y., Tian, G. and Wang, H. (2014), "Velocity effect analysis of dynamic magnetization in high speed magnetic flux leakage inspection", *NDT E Int*., **64**, 7-12. https://doi.org/10.1016/j.ndteint.2014.02.001
Wu, D., Zhang, Z., Liu, Z. and Xia, X. (2015), "3-D FEM simulation and analysis on the best range of lift-off values in MFL testing", *J. Test. Eval*., **43**(3), 673-680. https://doi.org/10.1520/JTE20130133
Zhang, Y., Ye, Z. and Wang, C. (2009), "A fast method for rectangular crack sizes reconstruction in magnetic flux leakage testing", *NDT E Int*., **49**, 369-375. https://doi.org/10.1016/j.ndteint.2009.01.006